Denoising of NIRS Measured Biomedical Signals

Y V Rami reddy[1], Dr.D.VishnuVardhan [2]
[1]M. Tech, Dept of ECE, JNTUA College of Engineering, Pulivendula, A.P, India
[2]Assistant Professor, Dept of ECE, JNTUA College of Engineering, Pulivendula, A.P, India
[1]ramireddy.ksrm@gmail.com, [2]vishnushreyan@gmail.com

Abstract— **Near-infrared spectroscopy (NIRS) is a non-invasive technique uses near-infrared light to measure changes in cerebral blood flow. The signals observed in this technique are well approximated with low-frequency, sparse or sparse derivative components, instrumental noise and motion-artifacts. In order to filter this type of signals one optimization approach and two algorithms namely LPF/TVD and LPF/CSD are developed in this paper. Here for enhanced sparsity total variation denoising and l_1 norm are used. For computational efficiency discrete-time zero-phase non causal recursive filters are used and are formulated in terms of banded matrices for finite length data.**

Keywords: NIRS, Sparse approximation, Total variation denoising (TVD), Low and high pass and zero-phase filters.

I. INTRODUCTION

The NIRS technique uses infrared light in the range of (690-1000) nm at two or more wavelengths. The transmission and absorption of NIR light in human body tissues contains information about hemoglobin concentration changes. On observation it is noted that the signals measured in this technique consist of sparse signal with instrumental noise, motion-artifacts and baseline drift in the low-frequency background [2]. Low frequency LTI filters are used to filter low-pass signals, total variation de-noising is used to filter sparse represented signals [1]. By using LTI filters the proposed NIRS measured signals are not recovered well. So to recover these types of signals both total variation de-noising and LTI filtering are effectively combined. The proposed signal y(n) is modeled as

$$y(n) = f(n) + x(n) + w(n),\ n = 0,1,\ldots,N-1 \quad (1)$$

Where f is a low-pass signal, x is a sparse and/or sparse derivative signal, and w is instrumental noise (approximately stationary white Gaussian noise). To filter the signals which are modeled in (1) an optimization approach is presented that combines the LTI and sparsity based denoising to extract a low-pass and a sparse signal from a single noisy additive mixture. Here first the sparse or sparse derivative component x is recovered by using two algorithms. If x were sparse derivative signal it is extracted using LPF/TVD algorithm which uses Majorization-minimization (MM) principle. If x were a sparse or sparse derivative signal it is derived using LPF/CSD algorithm which uses alternate direction of method of multipliers (ADMM). By subtracting the estimated x component from original signal and on applying the low-pass filter component f is obtained. First algorithm is special case of second algorithm so instead first one second algorithm can also be used, but the first algorithm converges faster than second one and also it doesn't require a step size parameter whereas second algorithm does.

For computational efficiency we design and describe a zero phase non causal recursive filters and are formulated in terms of banded matrices for finite length data. Here recursive filters are chosen for computational efficiency and the property zero-phase is chosen to avoid phase distortion. Causality is not necessary since algorithms are developed for processing in batch-mode.

II. PRELIMINARIES

A. Notation

The N-point signal *x* is denoted by the vector

$$\mathbf{x} = [x(0), \ldots, x(N-1)]^T \quad (1)$$

The l_p norm of a vector **x** is defined as

$$\|x\|_p = \left(\sum_{n=0}^{N-1} |x|^p\right)^{1/p} \text{ where p taken as } 0 < p \leq 1 \text{ for enhanced sparsity}$$

The l_2 norm of a vector **x** is defined as

$$\|x\|_2 = \left[\sum_n |x(n)|^2\right]^{\frac{1}{2}}$$

The matrix **D** is defined as

$$\mathbf{D} = \begin{bmatrix} -1 & 1 & & & \\ & -1 & 1 & & \\ & & \ddots & \ddots & \\ & & & -1 & 1 \\ & & & & -1 \quad 1 \end{bmatrix}. \quad (2)$$

Dx gives the first-order difference of an N-point signal **x**, where **D** is of size (N−1)×N).
The soft-threshold function [3] is denoted as

$$\text{Soft(x, T)} := \begin{cases} x - T\left({}^{x}/_{|x|}\right), & |x| > T \\ 0 & |x| \le T \end{cases}$$

The notation Soft(x, T) refers to the soft-threshold function operated element-wise to x for T > 0.

B. Total Variation Denoising

Let x be the sparse derivative signal is observed with instrumental noise (approximately additive white Gaussian noise) w

i.e., y = x+w

Estimation of signal x under noisy observation is called total variation denoising. l_1 Norm represents proxy operator for sparsity, so optimizing the l_1 norm of the derivative of x subject to a data fidelity constraint is named as sparse signal denoising. In discrete-time data, first-order difference gives the simplest approximation of the derivative; so, consider the minimization of $\| \mathbf{D}x_k \|_1$. Assume that the N-point signal x is observed with additive white Gaussian noise with variance σ^2, a proper data fidelity constraint is $\|y - x\|_2^{\,2} \le N\sigma^2$. This is called constrained optimization problem

$$arg \min_x \| \mathrm{D}x_k \|_1 \quad (3a)$$

$$\text{Such that } \|y - x\|_2^{\,2} \le N\sigma^2 \quad (3b)$$

It is equivalent for appropriate λ, to the unconstrained optimization problem

$$arg \min_x \{\frac{1}{2}\|y - x\|_2^{\,2} + \lambda \| \mathrm{D}x \|_1\} \quad (4)$$

i.e..

$$\underset{x}{\text{argmin}} \frac{1}{2}\sum_{n=0}^{N-1}|y(n) - x(n)|^2 + \lambda \sum_{n=1}^{N-1}|x(n) - x(n-1)|$$

The solution to problem (4) is denoted as tvd(y, λ),

$$\text{tvd(y}, \lambda) = arg \min_x \{\tfrac{1}{2}\|y - x\|_2^{\,2} + \lambda \| \mathrm{D}x \|_1\} \quad (5)$$

The solution is more nearly piecewise constant by increasing the parameter λ.

C. Fused lasso signal approximator

In the case both the signal x and its derivative are sparse, the denoising problem is formulated as below

$$\underset{x}{arg\,min} \{\tfrac{1}{2}\|(\boldsymbol{y} - \boldsymbol{x})\|_2^{\,2} + \lambda_0 \|x\|_1 + \lambda_1\|Dx\|_1\} \quad (6)$$

The above problem is a special case of compound penalty function [4], [5]. Here two regularizers are used to recover distinct properties of a signal. The above problem is stated as 'fused lasso signal approximator [6]. The solution to (6) is written as

$$\text{x= soft (tvd (y, } \lambda_1\text{), } \lambda_0\text{)} \quad (7)$$

D. Majorization-Minimization

Majorization-minimization (MM) is an approach to solve optimization problems that are too difficult to solve directly [7]. Instead of minimizing the cost function F (x) directly, the MM approach solves a sequence of optimization problems, G_k(x), k = 0, 1, 2,….: The idea is that each G_k(x) is easier to solve that F (x).The MM approach produces a sequence x_k, each being obtained by minimizing G_k(x). To use MM, one must specify the functions G_k(x). The trick is to choose the G_k(x) so that they are easy to solve, but they should also each approximate F(x).

The MM approach requires that each function G_k(x) is a majorizor of F (x), i.e.,

$$G_k(x) \ge F(x_k), \qquad \forall x$$

and that it agrees with F (x) at x_k, $\quad G_k(x) = F(x_k)$

In addition, $G_k(x)$should be convex functions.

The MM approach then obtains x_{k+1} by minimizing $G_k(x)$.

$$x_{k+1} = \underset{x \in R^N}{arg\,min}\ G_k(\boldsymbol{x}) \quad (8)$$

The majorizer for the l_1 norm is given below

$$\tfrac{1}{2}x^T \Lambda_k^{\,-1}\mathbf{x} + \tfrac{1}{2}\| x_k \|_1 \ge \| \mathbf{x} \|_1,\ \Lambda_k = diag(|x_k|) \quad (9)$$

With equality when x = x_k Therefore, the left-hand-side of (9) is a majorizer of $\| \mathbf{x} \|_1$ and we will use it as G(x) in the MM procedure. Equation (9) is a result of $(|x| - |x_k|)^2 \ge 0$ for x, $x_k \in R$

III. PROBLEM FORMULATION

Let consider the problem of NIRS biomedical signal is observed with noise is represented as,

$$y = f+x+w \tag{10}$$

where f is low pass signal and x is sparse or sparse derivative signal and w is stationary white Gaussian noise (approximation of instrumental noise) with variance σ^2 We seek estimates

$$\hat{x} \approx x, \ \hat{f} \approx f \tag{11}$$

The low-pass signal f will be estimated as

$$\hat{f} := LPF(y - \hat{x}) \tag{12}$$

Where LPF is a specified low-pass filter. Here, the problem is to estimate $\hat{x}$. We should choose $\hat{x}$ such that

$$LPF(y - \hat{x}) \approx f. \tag{13}$$

$$LPF(y - \hat{x}) \approx y - x - w \tag{14}$$

Using (11) in (14) gives

$$LPF(y - \hat{x}) \approx y - \hat{x} - w \tag{15}$$

or

$$y - \hat{x} - LPF(y - \hat{x}) \approx w \tag{16}$$

Note that in the above equation left-hand side term represents a high-pass filter of $y - \hat{x}$.
Defining HPF = I-LPF, equation (16) is written as

$$HPF(y - \hat{x}) \approx w \tag{17}$$

Using bold letter H the matrix of high-pass filter is represented as $H(y - \hat{x}) \approx w$. Hence, $\hat{x}$ is chosen such that $H(y - \hat{x})$ represents a white Gaussian random vector with variance σ^2 and also $\hat{x}$ should have a sparse derivative; i.e., the l_1 norm of Dx should be small. Therefore, the estimation of x of can be denoted as the constrained optimization problem

$$arg \min_x \| Dx \|_1 \tag{18a}$$

$$\text{Such that} \quad \|\boldsymbol{H}(\boldsymbol{y} - \boldsymbol{x})\|_2^{\,2} \leq \boldsymbol{N}\sigma^2 \tag{18b}$$

For suitable λ, an equivalent formulation is the unconstrained optimization problem:

$$\underset{x}{arg\ min} \{\frac{1}{2}\|\boldsymbol{H}(\boldsymbol{y} - \boldsymbol{x})\|_2^{\,2} + \lambda\|Dx\|_1\} \tag{19}$$

We refer (18) and (19) as the LPF/TVD problem, the unconstrained form is computationally easier to solve.
The high-pass filter H will be set in the form

$$H = A^{-1}B \tag{20}$$

where A and B are banded matrices, but A^{-1} is not, and hence neither is H. The low-pass filter LPF to estimate f in (12) will be given by LPF = I-HPF with filter matrix L = I- $A^{-1}B$.

IV. LPF/TVD ALGORITHM

In this section NIRS measured biomedical signal denoised by using MM procedure. Here first the sparse derivative component x is extracted by using MM concept then low-pass component f is obtained by applying low-pass filtering. The following change of variables is required to make the solution (18) unique and to provide subsequent use of MM . Let

$$x = Su \tag{21}$$

where S is a matrix of size N× $(N-1)$ of the form

$$\mathbf{S} := \begin{bmatrix} 0 & & & & \\ 1 & 0 & & & \\ 1 & 1 & 0 & & \\ \vdots & & & \ddots & \\ 1 & 1 & \cdots & 1 & 0 \\ 1 & 1 & \cdots & 1 & 1 \end{bmatrix} \tag{22}$$

It denotes a cumulative sum. Note that

$$DS = I \tag{23}$$

i.e., S is a discrete anti-derivative. So,

$$Dx = DSu = u \tag{24}$$

Note that for the filters to be described in Section vi the matrix B can be represented as

$$B = B_1 D \tag{25}$$

where B_1 is also banded matrix for the computational efficiency of the algorithm.
By using (21) problem (19) is written as

$$\underset{u}{arg\,min}\ \{F(u) = \frac{1}{2}\|H(y - Su)\|_2^{\,2} + \lambda \|u\|_1\} \tag{26}$$

The solution to (19) is obtained as x = Su by obtaining optimal solution to u. To minimize (26) using MM, we require a majorizer $G_k(u)$ of the cost function F(u) in (26). A majorizer of F(u) is given by using (9) as

$$G_k(u) = \frac{1}{2}\|H(y - Su)\|_2^{\,2} + \frac{\lambda}{2} u^T \Lambda_k^{\,-1} u + \frac{\lambda}{2} \| u_k \|_1$$

where Λ_k is the diagonal matrix,

$$[\Lambda_k]_{n,n} = |u_k(n)|$$

Using (20), (23) and (25),

$$HS = A^{-1}BS = A^{-1}B_1DS = A^{-1}B_1,$$

and the majorizer can be written as

$$G_k(u) = \frac{1}{2}\|A^{-1}By - A^{-1}B_1u)\|_2^{\,2} + \frac{\lambda}{2} u^T \Lambda_k^{\,-1} u + C$$

where C does not depends on u. The MM update is given by

$$u_{k+1} = \underset{u}{arg\,min}\ G_k(u) \tag{27}$$

In the explicit form the above update is written as

$$u_{k+1} = (B_1^{\,T}(AA^T)^{-1}B_1 + \lambda\ \Lambda_k^{\,-1})^{-1} B_1^{\,T}(AA^T)^{-1}By$$

A numerical problem is that, due to the sparsity promoting properties of the l_1 norm, many values of u_k will become zero as the iterations progress and hence some entries of $\Lambda_k^{\,-1}$ will go to infinity. So the above equation is rewritten using the matrix inverse lemma as

$$(B_1^{\,T}(AA^T)^{-1}B_1 + \lambda\ \Lambda_k^{\,-1})^{-1} = \frac{1}{\lambda}\Lambda_k - \frac{1}{\lambda}\Lambda_k B_1^{\,T}(\lambda AA^T + B_1\Lambda_k B_1^{\,T})^{-1} B_1\Lambda_k \tag{28}$$

In the above equation all the matrices A, B_1 and Λ_k are banded hence the above equation is banded. The MM update (27) can be implemented using (28) as:

$b \leftarrow \frac{1}{\lambda} B_1^{\,T}(AA^T)^{-1}By$
$\Lambda_k \leftarrow \mathrm{diag}(|u_k|)$
$u_{k+1} \leftarrow \Lambda_k[b - B_1^{\,T}(\lambda AA^T + B_1\Lambda_k B_1^{\,T})^{-1} B_1\Lambda_k b]$

The above equation is solved using banded system of linear equations and all multiplications are computationally efficient since all matrices are banded. From the above developed equations LPF/TVD algorithm can be written as

LPF/TVD Algorithm:

Input: $y \in R^N$, $\lambda > 0$
Output: $x, f \in R^N$

1: $b \leftarrow \frac{1}{\lambda} B_1^{\,T}(AA^T)^{-1}By$
2: $u \leftarrow Dy$
3: repeat
4: $\Lambda_k \leftarrow \mathrm{diag}(|u|)$
5: $Q \leftarrow \lambda AA^T + B_1\Lambda B_1^{\,T}$
6: $u \leftarrow \Lambda_k[b - B_1^{\,T}(Q)^{-1} B_1\Lambda b$
7: until convergence
8: $x \leftarrow Su$
9: $f \leftarrow (y - x) - A^{-1}B(y - x)$
10: return x, f

Change of variables x=Su in the MM approach leads to a reduction of number equations. Each iteration has O(dN) computational cost, where d is the order of the filter H.

Optimality Conditions: The optimality conditions characterizing the minimizer of (19) are taken from [8]. Define

$$g = S^T H^T H(y - x), u = Dx \tag{29}$$

Then x minimizes (19) if and only if

$$\begin{aligned} g(n) &= \mathrm{sign}(u(n)) \cdot \lambda, && \text{for } u(n) \neq 0 \\ |g(n)| &\leq \lambda, && \text{for } u(n) = 0 \end{aligned} \tag{30}$$

The above equation is used to verify optimality condition and also to set the $\lambda(\text{regularization parameter})$. Note that if y consists of noise only then x will be identically zero. From (29), g and u are given in this case by

g = $S^T H^T$Hw and u = 0 and. This is optimal, according to (30), if $\lambda \geq \max(g) = \max(S^T H^T \mathrm{Hw})$. Minimal λ is chosen to avoid unnecessary attenuation/distortion of, we get the value

$$\lambda = \max(S^T H^T \mathrm{Hw}) \tag{31}$$

In the case of noise is white Gaussian with zero-mean and variance σ^2 , then we may compute the standard deviation of $S^T H^T$Hw and use the 'three-sigma' rule in the place of maximum value.

$$\lambda = 3\mathrm{std}(\mathrm{S^T H^T Hw})$$

V. COMPOUND SPARSE DENOISING ALGORITHM (LPF/CSD)

Here we apply ADMM procedure to extract sparse or sparse derivative component, then we will apply low-pass filter to $(y - \hat{x})$ to estimate the low-pass component f, instead of solving (19), we solve

$$\underset{x}{\boldsymbol{arg\ min}} \{\frac{1}{2}\|\mathrm{H}(\boldsymbol{y} - \boldsymbol{x})\|_2^{\,2} + \lambda_0 \|x\|_1 + \lambda_1 \|Dx\|_1\} \tag{32}$$

which promotes sparsity of both x and its first-order difference. The high-pass filter H = $\mathrm{A^{-1}B}$ used is same as above, as it represents the behaviour of the low-pass component f. The problem (32) is referred as the LPF/CSD problem ('CSD' for compound sparse denoising) and it also referred as compound regularization [4],[5] since use of two regularizers. The terms of the cost function are separated by applying 'variable splitting' as in [13]. Here, problem (32) can be rewritten as

$$\underset{x,v}{arg\ min} \{\frac{1}{2}\|\mathrm{Hy} - \mathrm{Hx}\|_2^{\,2} + \lambda_0 \|x\|_1 + \lambda_1 \|Dx\|_1\} \tag{33a}$$

$$\text{Such that v = x} \tag{33b}$$

Applying ADMM to (33) results the iterative algorithm:

$$\mathrm{x} \leftarrow \underset{x}{arg\ min}\ \frac{1}{2}\|\mathrm{Hy} - \mathrm{Hx}\|_2^{\,2} + \mu\|\mathrm{v} - \mathrm{x} - \mathrm{d}\|_2^{\,2} \tag{34a}$$

$$\mathrm{v} \leftarrow \underset{v}{arg\ min}\ \lambda_0 \|v\|_1 + \lambda_1 \|Dv\|_1 + 0.5\mu\|\mathrm{v} - \mathrm{x} - \mathrm{d}\|_2^{\,2} \tag{34b}$$

$$\mathrm{d} \leftarrow \mathrm{d} - (\mathrm{v} - \mathrm{x}) \tag{34c}$$

$$\text{Go to (34a)} \tag{34d}$$

The algorithm (34) alternates between minimization with respect to x in (34a) and v in (34b) and parameter $\boldsymbol{\mu} > 0$ should be specified. Convergence behaviour of algorithm is varied based on the value of $\boldsymbol{\mu}$**.** The variables d and v also must be specified before entering into the loop; Both d and v are initialized to zero vectors of same length as y. Until satisfying some stopping criterion repetition loop is going on. The solution to (34a) is written as

$$\mathrm{x} \leftarrow (\mathrm{H^T H} + \mu\mathrm{I})^{-1}(\mathrm{H^T Hy} + \mu(\mathrm{v} - \mathrm{d})) \tag{35}$$

from H = $\mathrm{A^{-1}B}$ we write

$$\mathrm{H^T Hy} = \mathrm{B^T}(\mathrm{AA^T})^{-1}\mathrm{By} \tag{36}$$

By using the matrix inverse lemma, we get

$$(\mathrm{H^T H} + \mu\mathrm{I})^{-1} = \frac{1}{\mu.}[\mathrm{I} - \mathrm{B^T}(\mu\mathrm{AA^T} + \mathrm{BB^T})^{-1}\,\mathrm{B}] \tag{37}$$

Using (36) and (37) in (35), line (34a) is implemented as

$$\mathrm{g} \leftarrow \frac{1}{\boldsymbol{\mu}.}\mathrm{B^T}(\mathrm{AA^T})^{-1}\mathrm{By} + (\mathrm{v\text{-}d}) \tag{38a}$$

$$\mathrm{x} \leftarrow \mathrm{g} - \mathrm{B^T}(\boldsymbol{\mu}\mathrm{AA^T} + \mathrm{BB^T})^{-1}\,\mathrm{Bg} \tag{38b}$$

Observe that only once we have to compute the first term on the right-hand side of (38a), because y is not updated in the loop (34); so it can be pre-calculated prior to the iteration. The solution to (34b) can be written as v←soft(tvd(x+d, λ_1/μ),λ_0/μ) The complete algorithm is called as Algorithm 2.

LPF/CSD Algorithm:

Input: y∈ $\mathrm{R^N}$, $\lambda_0 > 0$, $\lambda_1 > 0$, $\mu > 0$

Output: x, f ∈ $\mathrm{R^N}$

1: v←0
2: d←0
3: b← $\frac{1}{\mu.}\mathrm{B^T}(\mathrm{AA^T})^{-1}\mathrm{By}$
4: repeat
5: g←b+v−d
6: x←g− $\mathrm{B^T}(\mu\mathrm{AA^T} + \mathrm{BB^T})^{-1}\,\mathrm{Bg}$
7: v←soft(tvd(x+d, λ_1/μ),λ_0/μ)
8: d←d−v+x
9: until convergence
10: f← (y − x) − $\mathrm{A^{-1}B}$(y − x)
11: return x, f

VI. DESIGN OF FILTERS

In this section discrete-time zero-phase non causal recursive filters are designed. We represent the discrete-time filter by the difference equation

$$\sum_k a(k)y(n-k) = \sum_k b(k)x(n-k) \tag{39}$$

Where x(n) and y(n) represents input and output signals respectively. Its frequency response is given by

$$H(e^{jw}) = \mathbf{B}(e^{jw})/ A(e^{jw})$$

For finite length signals the difference equation (39) is implemented in matrix form as

$$Ay = Bx$$

Where A and B are banded matrices. Filter output y is written as

$$y=A^{-1}Bx \tag{40}$$

If we apply this filter to finite length signals there will be start and end- transients. To minimize start transients initial states of the filter must be specified, if not are usually taken as zero or optimized.

A. Zero-phase filters

The filter should be zero-phase to avoid unnecessary distortion. The conditions required to meet zero-phase property are 1. Frequency response is real valued or impulse response is symmetric, 2. Filter should behave same 'backwards' as it does 'forwards' i.e. applying the filter H to the reversed version of x, then reversing the filter output should be same as the output of the filter obtained by applying directly to x . Let J denote the reversal matrix, the filter should satisfy

$$JHJ = H \tag{43}$$

where the size of J is determined by the dimensions of H

If A and B satisfy

$$JAJ = A \text{ and } JBJ = B, \tag{44}$$

then $H = A^{-1}B$ satisfies (43)

The filter matrices present in proposed LPF/TVD algorithm, should satisfy (43).

VII RESULTS

A. Filters Design Result

While developing the above algorithms filters are designed to meet a zero phase property. Those filter results are shown below. From the below results it is observed that filters have a real valued frequency response and symmetric impulse response. So filters satisfied zero-phase property.

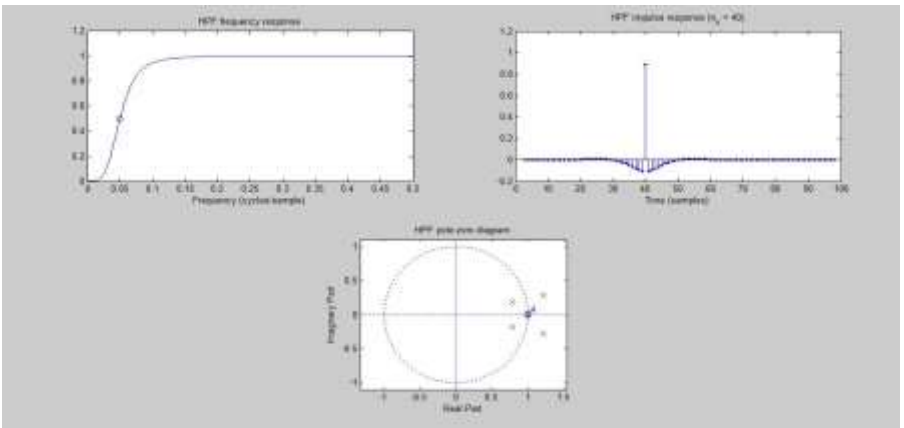

Fig 1 High-pass non-causal 2nd order filter with cut-off frequency $\omega_c = 0.1\pi$

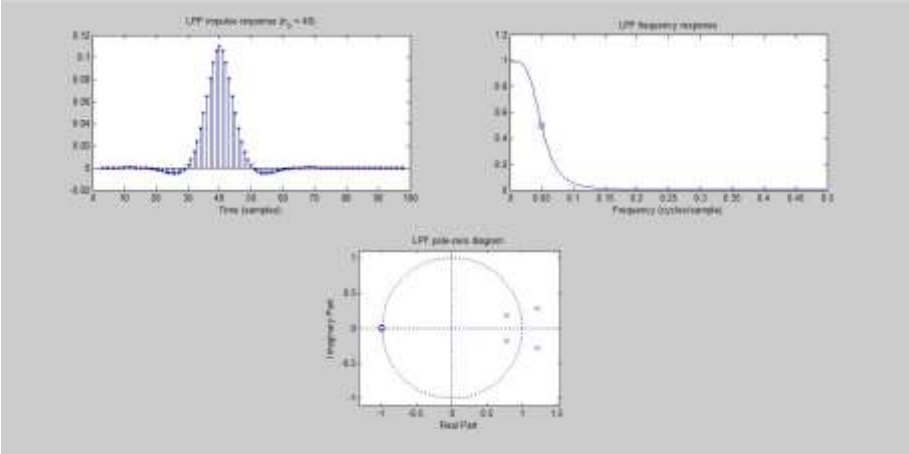

Fig 2 low pass non-causal 2nd order filter with cut-off frequency $\omega_c = 0.1\pi$.

B. LTI (Low-pass) filtering result

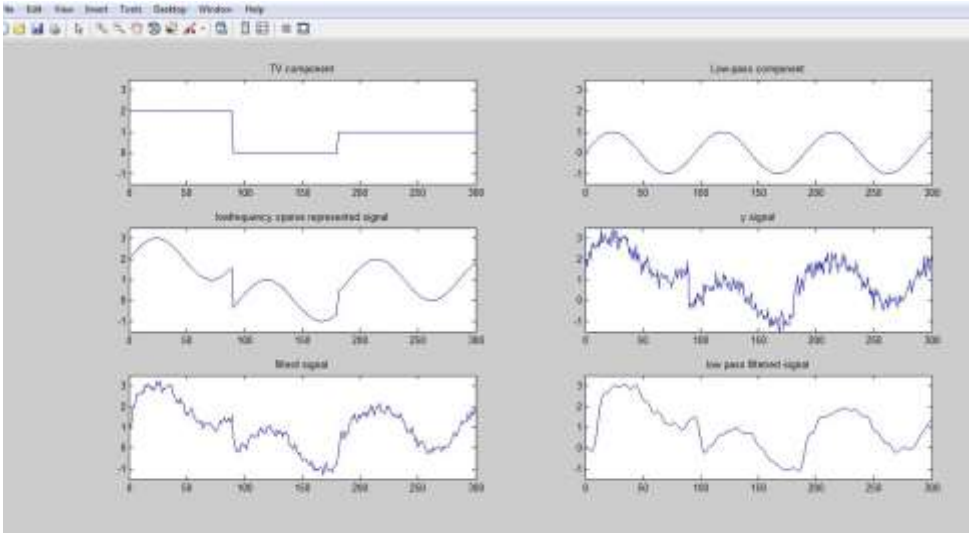

Fig 3 LTI filtering result showing the proposed signal is not recovered well

In the above result low frequency sparse represented signal with instrumental noise (approximately Gaussian noise) designed. After applying low-pass filtering to the above signal it is observed that the signal is not recovered well.

C. LPF/TVD algorithm result for the above designed signal.

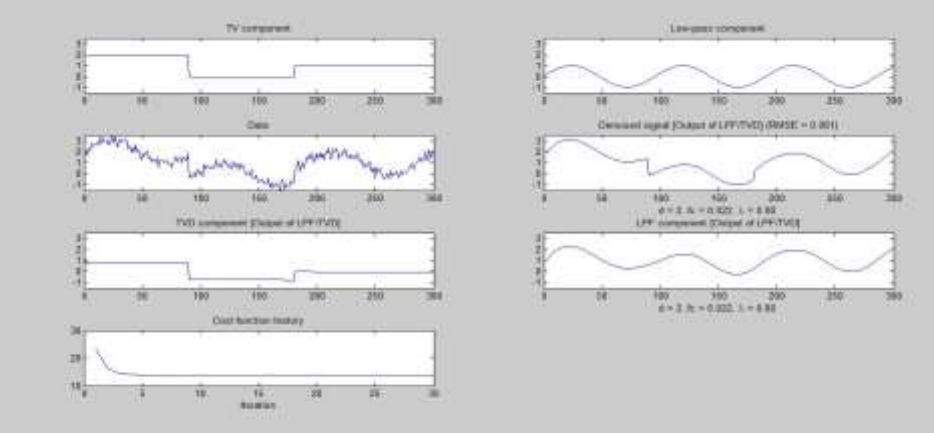

Fig 4a Denoising of low-frequency sparse represented signal using LPFTVD algorithm with parameters $\lambda = 0.8$, d= 2, $\omega_c = 0.044\pi$.

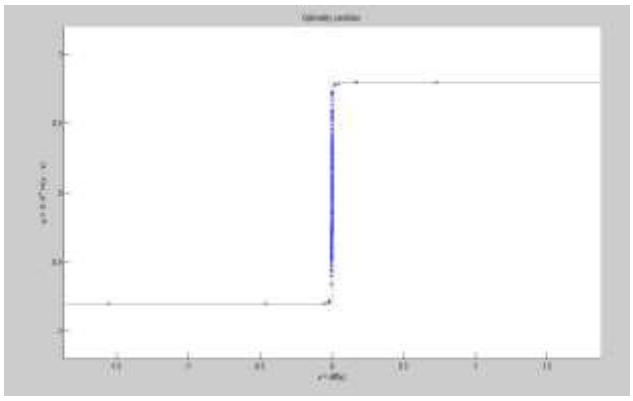

Fig 4b verification of optimality condition using scatter plot for LPFTVD algorithm

After applying LPFTVD algorithm to the above designed signal it is observed that it decomposes the signal into low-pass and TVD components and also observed that signal is recovered well compare to the low-pass filtering. Fig 6.4b illustrates that plot between variables g and u lies on the step function according to the conditions in (29), (30). So the cost function for solving sparse derivative component is minimized.

D. LPFTVD algorithm result to the NIRS time series measured data.

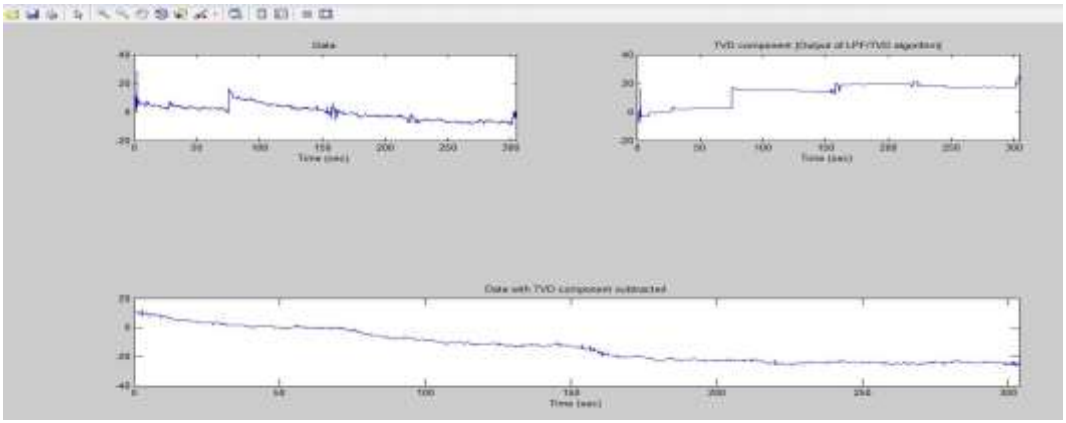

Fig 5a. Removal of abrupt changes of baseline and transient artifacts from NIRS time series measured data using LPF/TVD algorithm with parameters $\lambda = 1.2$, $d = 1$, $\omega_c = 0.04\pi$

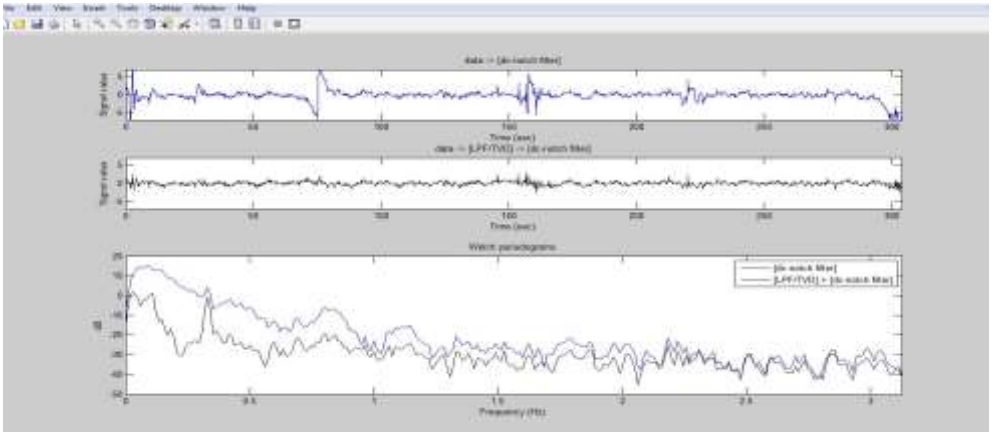

Fig 5b Comparison of output of LTI de-notch filtering and LPFTVD algorithm processed data and periodogram for LPFTVD algorithm obtained data reveals the signal component at 0.32Hz frequency which is unnoticed by the wide low-frequency energy because of strong transients.

In the above results brain signal measured for 304 seconds by keeping NIRS equipment on back of the head and subjecting to motion artifacts. Due to motion approximately at 80 second mark base line valve is shifted. On

applying LPF/TVD algorithm TVD component is obtained. This component captures transient artifacts and discontinuities in the signal.

From fig 6.4b it is observed that on applying de-notch filtering on the data, base line shift removed but transient artifacts are present in the data. These baseline shift and transient artifacts are removed effectively by subtracting the TVD component from the data prior to the de-notch filtering. Periodogram for LPF/TVD algorithm obtained data reveals the signal component at 0.32Hz frequency which is which is unnoticed by the wide low-frequency energy because of strong transients. So LPF/TVD processing is also useful for spectral analysis.

E. LPF/CSD algorithm result of NIRS time series measured data

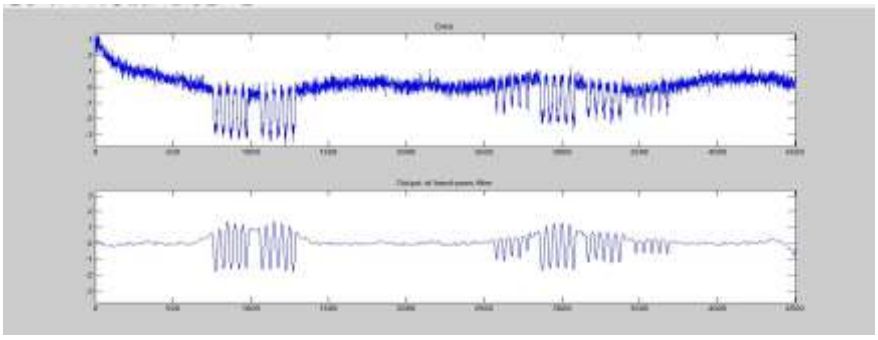

Fig 6a Output of band-pass filter to NIRS time series measured data.

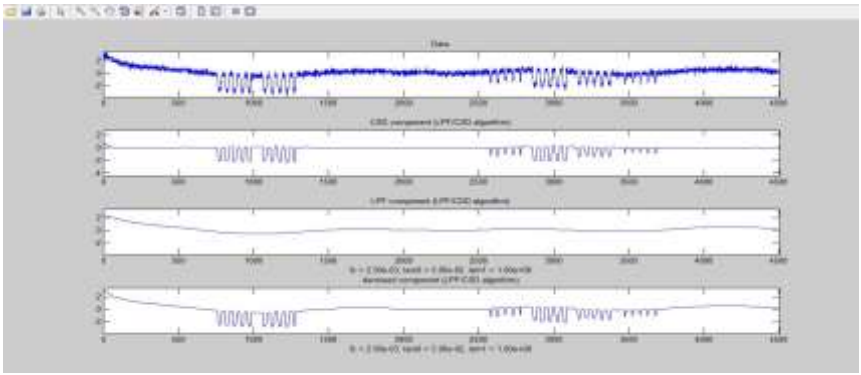

Fig 6b LPF/CSD algorithm output for NIRS time series measured data.

In the above figures data is collected from dynamic tissue-simulating phantom represents the hemodynamic response of a human brain. The signal is measured for 3602 seconds duration with sampling rate of 1.25 samples per second. Data consists of low-frequency component, hemodynamic pulses and wideband noise.

On applying band-pass filtering to the above measured data it is observed that baseline drifted, signal shape is not recovered well and smooth curve is not obtained.

On applying developed LPF/CSD algorithm with parameters N = 100, u = 0.4, $\lambda_0 = 0.05, \lambda_1 = 1$ for the above measured data it is observed that smooth curve is obtained preserving the shape of the pulses.

F. Comparison of convergence behavior of LPF/TVD and LPF/CSD algorithms.

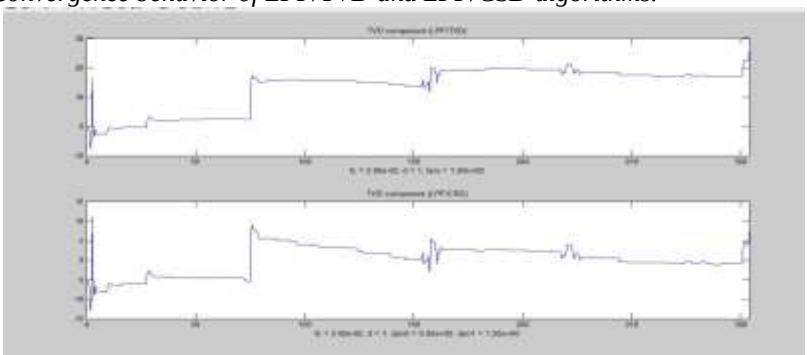

Fig 7a TVD component output obtained by LPF/TVD and LPF/CSD algorithms

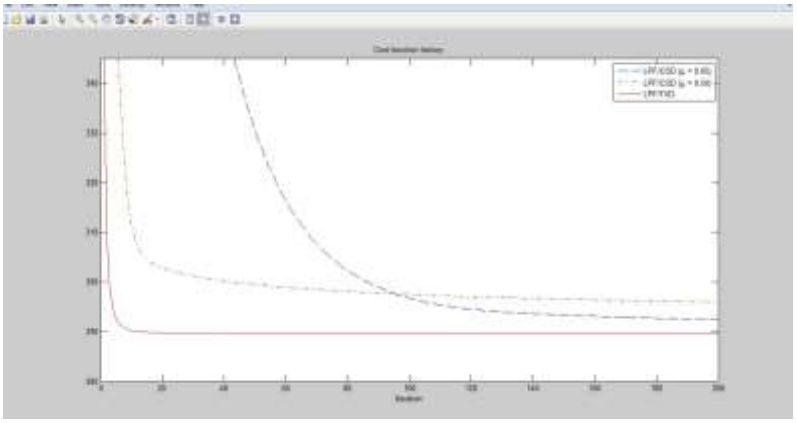

Fig 7b Comparison of convergence behavior of LPF/TVD and LPF/CSD algorithms

From the figure 6.7a it is observed that TVD component obtained by LPF/CSD algorithm with parameters u =0.4, $\lambda_0 = 0, \lambda_1 = 1$ is same as the TVD component obtained by LPF/TVD algorithm. Only the difference is the LPF/CSD algorithm requires the specification of parameter u.

From the figure 6.6b it is observed that LPF/TVD requires less number of iterations and there is no requirement specification of the parameter u compared to LPF/CSD algorithm. It is also observed that for LPF/CSD algorithm for u = 0.05 initial convergence is very poor but final convergence is good compared to u = 0.5 and for u = 0.5 initial convergence is good but final convergence is poor compared to u = 0.05.

G. Removal of artifacts from NIRS series measured data using LPF/CSD algorithm.

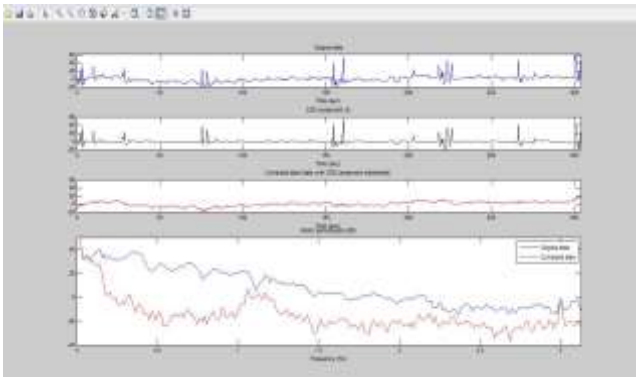

Fig 8. Removal of artifacts from the NIRS series measured data using LPF/CSD algorithm

In the above figure NIRS time series data measured for 304 seconds. Data consists of transient artifacts. On applying LPF/CSD algorithm on the data CSD component x is obtained. By subtracting CSD component from the data transient artifacts are removed and oscillatory behavior of the data is preserved. Periodogram for LPF/TVD algorithm processed data reveals the broad peak in the 1-1.2Hz frequency which is unnoticed by the wide low-frequency energy because of strong transients. So LPF/TVD processing is also useful for spectral analysis.

VIII CONCLUSION AND FUTURESCOPE

Generally LTI filtering is suitable to denoise the low-frequency signals and total variation denoising is suitable to filter sparse represented signals. On application of LTI filtering alone on the low-frequency sparse represented NIRS measured biomedical brain signals, the signals are not recovered well and also artifacts and baseline drift in the signal are not removed. In the proposed algorithms LPF/TVD and LPF/CSD, low-pass filtering and sparsity based denoising are effectively combined and application of these algorithms on the proposed signal showed that signals are effectively denoised and removed the artifacts, baseline drift in the proposed signal. The proposed algorithms can also be applied to the fields biology, audio signals etc., which having sparse representation in the low-frequency background. Powerful convex optimization approaches can also be developed based on proximity operators ([9],[10],[11]). In place of first order derivative higher order

derivatives and reweighted l_1 minimization [12] can also be used for enhanced sparsity and adaptive filtering techniques also be used to recover the sparse signals.

REFERENCES

[1] L. Condat. A direct algorithm for 1-D total variation denoising. IEEE Signal Processing Letters,20(11):1054–1057, November 2013.
[2]The odore J. Huppert, Solomon G. Diamond, Maria A. Franceschini, and David A. Boas. A review of time-series analysis methods for nearinfrared spectroscopy of the brain
[3] D. L. Donoho. De-noising by soft-thresholding. IEEE Trans. Inform.Theory, 41(3):613–627, May 1995.
[4] M. V. Afonso, J. M. Bioucas-Dias, and M. A. T. Figueiredo. An augmented Lagrangian approach to linear inverse problems with compound regularization. In Proc. IEEE Int. Conf. Image Processing, pages 4169–4172, September 2010.
[5] J. M. Bioucas-Dias and M. A. T. Figueiredo. An iterative algorithm for linear inverse problems with compound regularizers. In Proc. IEEE Int. Conf. Image Processing, pages 685–688, October 2008.
[6] J. Friedman, T. Hastie, H. H¨ofling, and R. Tibshirani. Pathwise coordinate optimization. Ann. Appl. Statist., 1(2):302–332, 2007.
[7] M. Figueiredo, J. Bioucas-Dias, and R. Nowak. Majorization minimization algorithms for wavelet-based image restoration. IEEE Trans. Image Process., 16(12):2980–2991, December 2007.
[8] [22] J.-J. Fuchs. On sparse representations in arbitrary redundant bases. IEEETrans. Inform. Theory, 50(6):1341–1344, 2004.
[9] L. M. Brice˜no-Arias and P. L. Combettes. A monotone+skew splitting model for composite monotone inclusions in duality. SIAM J. Optim., 21(4):1230–1250, October 2011.
[10] A. Chambolle and T. Pock. A first-order primal-dual algorithm for convex problems with applications to imaging. J. Math. Vis., 40(1):120–145, 2011.
[11] P. L. Combettes and J.-C. Pesquet. Primal-dual splitting algorithm for solving inclusions with mixtures of composite, Lipschitzian, and parallel-sum type monotone operators. Set-Valued and Variational Analysis, 20(2):307–330, June 2012.
[12] E. J. Cand`es, M. B. Wakin, and S. Boyd. Enhancing sparsity by reweighted reweighted l_1 minimization minimization. J. Fourier Anal. Appl., 14(5):877–905, December 2008.
[13] M. V. Afonso, J. M. Bioucas-Dias, and M. A. T. Figueiredo. Fast image recovery using variable splitting and constrained optimization. IEEE Trans. Image Process., 19(9):2345–2356, September 2010.